Characteristics of GaAs Spike Doped Collectors

P. J. Zampardi, K. Kwok, C. Cismaru, M. Sun, and A. Lo

***Abstract*—Spike-doped collector designs have recently been studied in both Si BJT and GaAs HBTs as a way to improve the device linearity while still maintaining ruggedness. In this work, we present and discuss – for the first time – the very interesting output characteristics of these devices (unique Ic-Vce curves) and how they are influenced by the device design. We also explore the improvement in cut-off frequency versus current and application of these devices to actual power amplifiers and the resulting changes in ruggedness.**

***Index Terms*—GaAs HBT, breakdown, collector design, power transistor**

I. Introduction

THE use of a non-uniform collector doping consisting of high-doped spike in the collector region has been demonstrated to improve the small-signal linearity in Si bipolar transistors [1]. More recently, similar structures have been demonstrated in III-V based transistors [2, 3], also showing an improvement in small-signal linearity. However, in power amplifier applications, linearity (especially small-signal single stage linearity) is not the only important metric. As was demonstrated in the work of Kim[4] that showed punch-through collectors gave linearity improvements at small signal, but these improvements disappeared at higher power levels. While [3] showed some device level improvements, no prior work has discussed use of these materials in an actual PA that shows the trade-offs among key parameters.

In this work, we discuss some of the interesting properties of these devices, especially the breakdown characteristics, the AC performance (from the current-gain cut-off frequency, f_T), and highlight some of the device design trade-offs. We then present circuit performance and ruggedness data.

II. Experimental Work

A. Description of Samples

The collector designs used in this study are shown in Table I. The structures studied include step doped collectors of 0.3, 0.55, 0.8 µm (structures A, B, C) and spike doped collectors (structures D, E, F) with a $2x10^{18}cm^{-3}$ 100Å spike at those positions, and a uniformly doped 1.1 um collector (structure G). The total collector lengths were kept the same. Two other structures, from and older run, are included with similar spikes at 0.3 and 0.45 and a total collector length of 0.8µm. The materials were grown by MOCVD by Kopin Corporation and processed through our standard HBT process.

P.J. Zampardi, K. Kwok, C. Cismaru, M. Sun, and A. Lo are with Skyworks Solutions, 2427 W. Hillcrest Drive, Newbury Park, CA 91320

Structure	Doping (cm^{-3}), Thickness (µm)		
	Collector I	Spike	Collector II
A	7.5e15, 0.3	N/A	3.0e17, 0.8
B	7.5e15, 0.55	N/A	3.0e17, 0.55
C	7.5e15, 0.8	N/A	3.0e17, 0.3
D	7.5e15, 0.3	2.0e18, 0.01	7.5e15, 0.79
E	7.5e15, 0.55	2.0e18, 0.01	7.5e15, 0.54
F	7.5e15, 0.8	2.0e18, 0.01	7.5e15, 0.29
G	7.5e15, 1.1	N/A	N/A

Table I – Collector structures

B. DC Characteristics

In order to compare the materials, the same size device (emitter area of 5.3 μm^2) was measured on each wafer. To evaluate the breakdown characteristics, BV_{ceo} and BV_{cbo} were measured, along with BV_{cex} measured as described in [5]. Fig. 1 shows that similar BV_{ceo} 's (or BV_{cbo}'s) were obtained for the step doped and spike doped collectors of which the spike and step are placed at the same location.

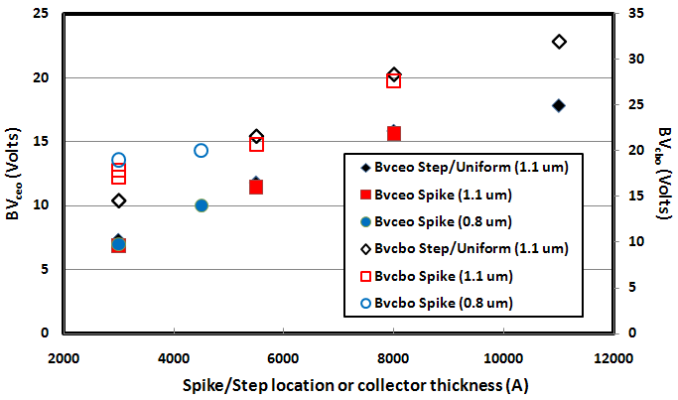

Fig. 1 – BV_{ceo} and BV_{cbo} for different spike/step positions and 1.1 um uniformly doped structure (note: circles are for spike doped structures in a 0.8 um collector).

The BV_{cbo} result stems from the fact that the spike is doped heavily so that the field drop in the spike is significant. Following [6], neglecting high-current effects but assuming a linearly decreasing electric field in the regions before and after the spike, we would expect:

$$\frac{V_{SD}}{V_B} = \left(\frac{W}{b}\right)^2 \left[\left(1 - \frac{\Delta E}{E_M} + \frac{2b}{W}\frac{\Delta E}{E_M}\right) \Big/ \left(\frac{2W}{b} - 1 + \frac{\Delta E}{E_M}\right)\right] \quad (1)$$

where V_{SD} is the spike dope breakdown, V_B is step dope breakdown, b is the spike/step position, E_M is the max electric field, ΔE is the electric field drop at the spike/step location, and W is the depletion length in the spike doped collector.

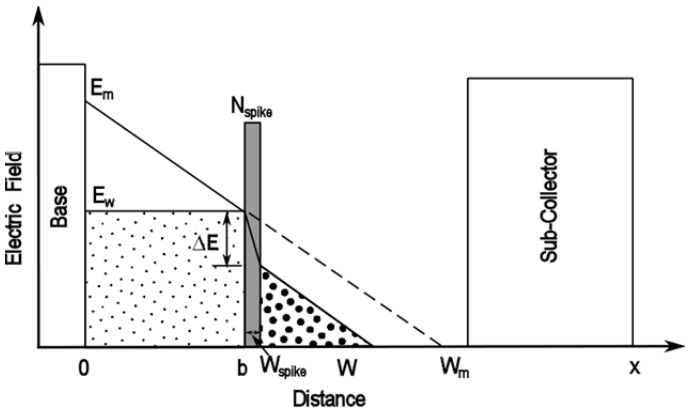

Fig. 2 – Schematic of electric field profile across collector

The large ΔE drop (see Fig. 2) was verified by simulation and explains why the spike and step BV_{cbo}'s are the same (from Eqn. (1), as ΔE → E_M, V_{SD} → V_B). The BV_{cex} measurements, shown in Fig. 3 show a splitting in BV_{cex} as the collector is shortened or the step/spike is moved closer to the base, where the spike doped collector has increased BV_{cex}. BV_{cex} is the point at which maximum V_{ce} occurs as shown in Fig. 4. The values for the spike doped samples are similar to the 1.1µm uniform collector, as we might expect if the field reaches all the way across the collector. The two older samples show a slightly lower BV_{cex} – even lower than the 8000A step doped. This is most likely due to the lower effective spike doping observed in the CV profiles. Fig. 4 shows the J_c vs. V_{ce} curves to help better understand the observations of Fig. 3. These are the zero base current "BV_{cex}" curves. The most interesting feature of these curves is that, as the spike is moved closer to the base, the collector current rises, then flattens out again. This feature was not reported in any of the prior work on spike doped collectors. As the spike is placed further from the base, the flattening out becomes less dramatic, but does delay the current from snapping back. The first rise (which normally gets interpreted as BV_{ceo}) only depends on the spike placement (collector thickness). Comparing the two 3000A spike doped structures, with slightly different peaks, we see that the current at which the current flattens out is dependent on the spike doping (as well as the placement) – so these breakdown curves can be tailored depending on the application. The explanation for this behavior is that as the current increases, the depletion edge will eventually punch-through the spike, allowing the overall field to lower, as discussed in [1]. Graphically, we can see this by overlaying the current-voltage curve with the doping vs. voltage. What we observe is that the flattening of the current for the spike dope occurs at the voltage for which the depletion edge passes through the spike doping, as shown in Fig. 5. This can also be observed by examining the base-emitter voltage (V_{be}) vs. V_{ce}. V_{be} increases due to avalanche current (to compensate for the holes entering the base due to breakdown) and decreases because of self-heating. Fig. 6 shows the V_{be} rises at BV_{ceo} because of breakdown then begins flattening out at the voltage which corresponds to the depletion edge passing through the peak of the spike. The doping profiles for the spike structures are overlaid with the V_{be} to emphasize this point.

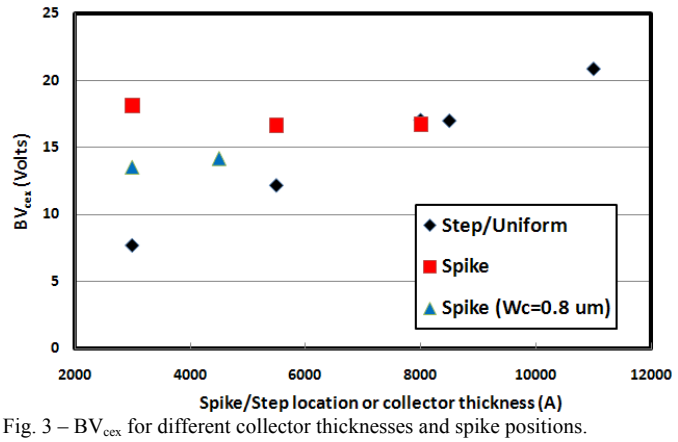

Fig. 3 – BV_{cex} for different collector thicknesses and spike positions.

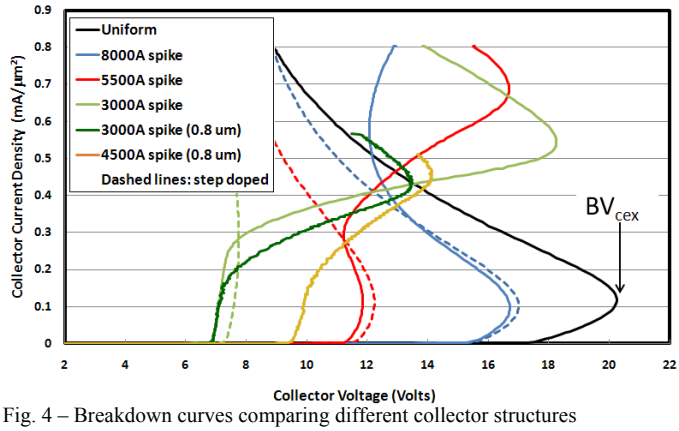

Fig. 4 – Breakdown curves comparing different collector structures

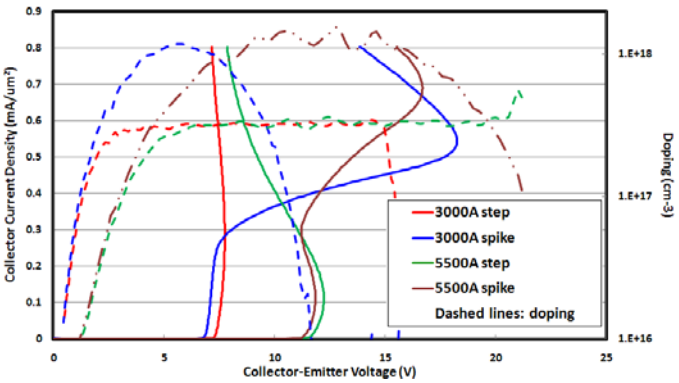

Fig. 5 – Comparison of doping profile vs. voltage with where the breakdown current increases for 3000A and 5500A step and spike samples.

To summarize the DC characteristics, spike position determines where the BV_{ceo} is and the spike peak doping and position determine the position of the spike punch-through. The BV_{cex} is primarily determined by the total collector thickness. Varying these parameters allow the collector breakdown current to be controlled.

C. AC Characteristics

First, we compare the collector-current cut-off frequency, f_T, characteristics. The important parameters are the peak f_T and the current density at which the peak occurred ($J_{c,peak,fT}$). Fig. 7 shows these parameters plotted vs. collector length (spike position). What we observe is that as the spike doping is moved towards the sub-collector, both the peak f_T and the critical current density for the spike and step dopings are very

similar and increase as the spike (step) is moved closer to the base (relative to the 1.1µm collector). We see that the 0.3um spike does not increase as much as the 0.3µm step doping. To understand this, we use the Kirk effect formula [7]:

$$J_{Kirk} = v\left\{qN_c + 2\varepsilon\left(V_{BC}+V_{bi}\right)/W_c^2\right\} \quad (2)$$

This equation is applicable to the step or uniform doped collectors. For the spike doped case, we modify Eqn. (2) from [8], by eliminating the heterojunction related terms. This gives:

$$J_{Kirk,spike} = qv\left\{N_C + \frac{2\varepsilon(V_{BC}+V_{bi})}{qW_c^2} + (N_S - N_C)\frac{2W_s\left(W_C - W_d - W_s/2\right)}{W_c^2}\right\} \quad (3)$$

Where we assume V_{bi}=1.2, V_{bc}=0.3, v=1.2x10^7 cm/s. N_s is the spike doping, N_c is the normal collector doping, W_d is the position of the spike, and W_s is the spike width. q is the electron charge and ε is the dielectric constant (=13.1). The resulting calculated values are shown on Fig. 7. There is excellent agreement for the uniform/step doped collectors. For the spike doped collectors, there is good qualitative agreement that shows that for the spike doped devices, the critical current should not rise as steeply for a step doped or uniform doped, short collector. From Eqn. 3, we note that the critical current density is sensitive to the spike doping and increasing the spike doping will increase the critical current.

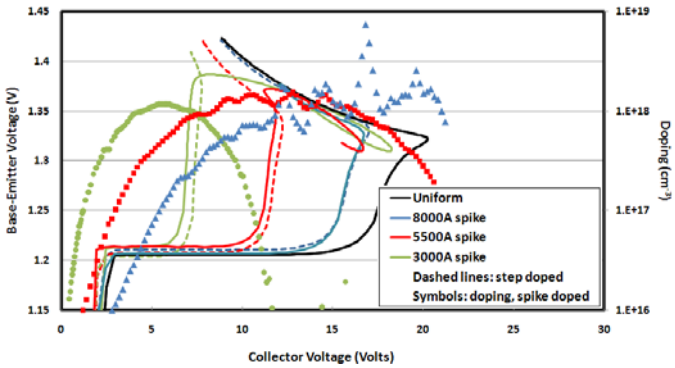

Fig. 6. Overlay of the measured Vbe and the doping profile calculated from CV measurement vs. collector voltage in breakdown and CV measurements (the doping profile voltage has been adjusted by 1.3 volts to convert from Vbc to Vce). Only the doping for spike doped samples are shown for clarity.

III. Circuit Performance

To study the effect of these collector designs on circuit performance, we built ~200 WCDMA power amplifier front-end modules (FEMs) from each of the wafers. The PA architecture is similar to [9] and includes a duplexer in the module. Fig. 8 shows the "figure of merit", ACP1+PAE, across the different materials. The testing was performed using automated production test and the parts were NOT retuned for performance. The step collectors show improved performance compared to the corresponding spike doped collectors in all three cases. There is a noticeable degradation in the FOM as the thickness of collector II increases as well. This is counter to what has been observed on *a device level* for linearity [2] where a shorter collector improved the linearity. Fig. 9 shows the measured gain for the FEMs. We see a modest difference in gain between the spike and step collectors. Again we note a steep fall-off in the gain for spikes or steps closer to the base. This is most likely due to the increased C_{bc} that the device encounters, due to the shorter collector, directly degrading the RF gain.

Besides the performance of the PAs, it is interesting to evaluate the benefit these material designs may provide for ruggedness. To evaluate this, we tested several parts from each material spec at -30C, as follows, until catastrophic failure: i) for each input power level (P_{in} = 5, 10, 15 dBm), different collector voltage V_{cc} (3.4, 4.6, 6 Volts) were applied, ii) for each combination of P_{in} and V_{cc} , the phase angle was increased from 0 to 340 degrees in 20 degree steps. We found that the spike doped structures D and F are more rugged than their step doped counterparts A and C. Most step doped structure B we tested are less rugged than the spike doped counterpart E. However, one part of the structure B was as rugged as the spike doped E parts. This exception could be caused by some part-to-part variation during assembly. Among the spike doped structures, the closer the spike is to the base, the more rugged the structure is. This data shows reasonable correlation between the PA ruggedness and the device-level BVcex (Fig. 3) together with the current flattening (Fig. 4) at least for this particular PA. We also note that the ruggedness data is consistent with trend that the spike doped structures have a lower gain than their step doped counterparts (Fig. 9). Finally, we found that the structure G (1.1 µm uniform collector) is less rugged than the spiked

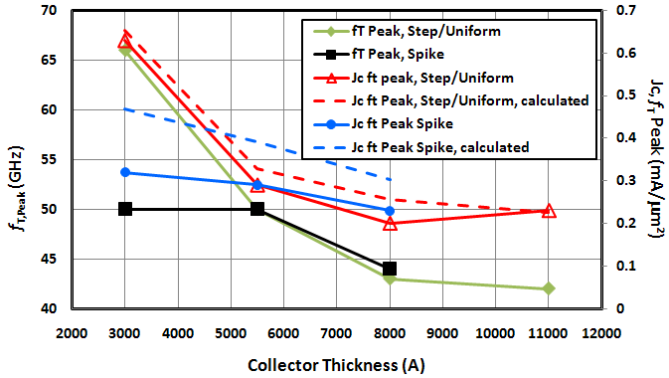

Fig. 7 – Peak f_T ($f_{T,Peak}$) and critical current ($J_{c,fT,Peak}$) for step/uniform and spike doped collectors. The position of the spike is used as the collector thickness for the spike doped samples.

doped structures D and E but as rugged as the spike doped structure F.

IV. Conclusion

In this work we demonstrated, for the first time, the unique breakdown characteristics for GaAs HBTs with spike doped collectors and discussed what collector design features control this behavior. The spike doping and placement both play key roles in this behavior. We also discussed the increase in critical current density, compared to just shortening the collector, for these structures and demonstrated good agreement between measured data and simple calculations. Finally, we demonstrated and compared these materials in a

power amplifier application. This data indicates that the improvement in device level linearity does not necessarily lead to circuit level linearity improvements. We also observed that the spike doped structures are more rugged than their step doped counterparts in handset applications.

ACKNOWLEDGMENT

We would like to acknowledge Megan Xu for providing product support, Shiaw Chang for providing the test circuit, and Hal Banbrook for much of the device level testing, and Rudy Vasquez and Luda Tereshchenko for the ruggedness testing. We would also like to thank Wibo van Noort for many interesting conversations about these devices.

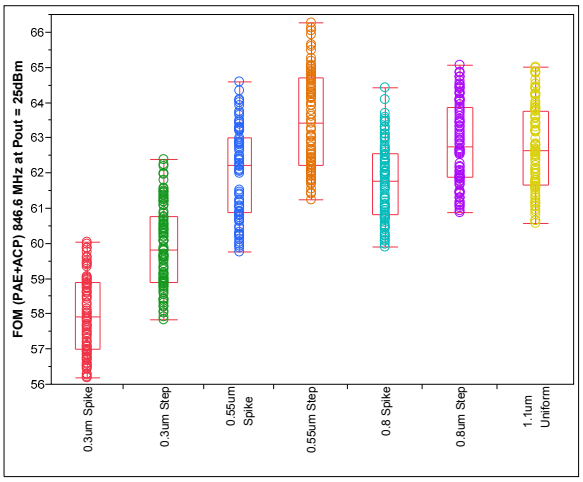

Fig. 8 – Figure of Merit (ACP1+PAE) for FEMs fabricated from different materials.

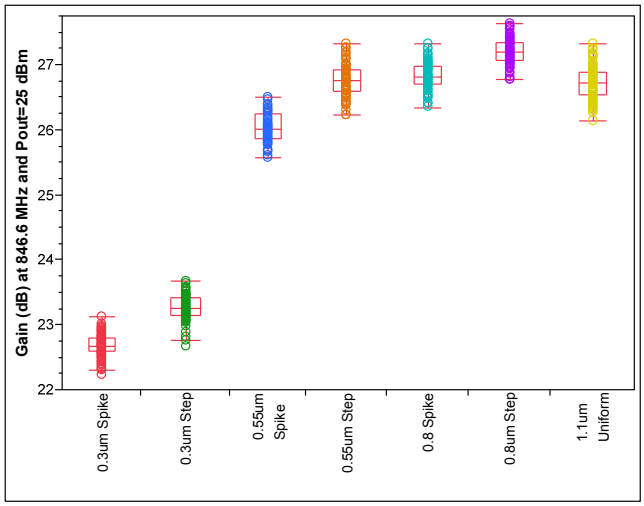

Fig. 9– Gain for FEMs fabricated from different materials

REFERENCES

[1] W. D. van Noort, L. C. N. de Vreede, H. F. F. Jos, L. K. Nanver, and Jan W. Slotboom, "Reduction of UHF Power Transistor Distortion With a Nonuniform Collector Doping Profile," *IEEE Journal of Solid-State Circuit*, Vol. 36, No. 9, Septemer 2001, pp. 1399-1406

[2] C. Wang, H-T Hsu, H. C. Shu, and Y. Hsin, "High Linearity InGaP/GaAs Power HBTs by Collector Design," *IEEE Electron Device Letters*, Vol. 25, No. 2, February 2004, pp. 58-60

[3] M-C Tu, H-Y Ueng, and Y-C Wang, "Performance of High-Reliability and High-Linearity InGaP/GaAs HBT PAs for Wireless Communication," *IEEE Transactions on Electron Devices,* Vol. 57, No. 1, January 2010, pp. 188-194

[4] W. Kim, S. Kang, K. Lee, M. Chung, Y. Yang, and B. Kim, "The Effects of C_{bc} on the Linearity of AlGaAs/GaAs Power HBTs," *IEEE Transactions on Microwave Theory and Techniques,* Vol. 49, No. 7, July 2001, pp. 1270-1276.

[5] C. Cismaru, H. Banbrook, and P.J. Zampardi, "High Volume Test Methodology for HBT Device Ruggedness Characterization," 2010 CS Mantech Conference, Paper 5.1

[6] S.M. Sze, Physics of Semiconductor Devices, 2nd Edition, New York, John Wiley & Sons, 1981, pg. 572.

[7] J. L. Moll, Physics of Semiconductors, New York, McGraw Hills, 1964, pp.154-155.

[8] W. Liu and D.S. Pan, "A Proposed Collector Design of Double Heterojunction Bipolar Transistors for Power Applications," *IEEE Electron Device Letters,* Vol. 16, No. 7, July 1995, pp. 309-311

[9] US Patent 7,486,134, "High efficiency load insensitive power amplifier"